Journal of Chromatography A, 1217 (2010) 7448–7454

Contents lists available at ScienceDirect

Journal of Chromatography A

journal homepage: www.elsevier.com/locate/chroma

Amphiphilic silica nanoparticles as pseudostationary phase for capillary electrophoresis separation

Hui Li[a], Guo-Sheng Ding[b,c], Jie Chen[a], An-Na Tang[a,*]

[a] Research Center for Analytical Sciences, College of Chemistry, Nankai University, 94 Weijin Road, Tianjin 300071, China
[b] Analysis Center, Tianjin University, 92 Weijin Road, Tianjin 300072, China
[c] School of Pharmaceutical Science and Technology, Tianjin University, 92 Weijin Road, Tianjin 300072, China

ARTICLE INFO

Article history:
Received 10 June 2010
Received in revised form
14 September 2010
Accepted 15 September 2010
Available online 18 October 2010

Keywords:
Silica nanoparticles
Amphiphilic
Capillary electrophoresis
Pseudostationary phase

ABSTRACT

Amphiphilic silica nanoparticles surface-functionalized by 3-aminopropyltriethoxysilane (APTES) and octyltriethoxylsilane (OTES) were successfully prepared and characterized using scanning electron microscopy (SEM), transmission electron microscopy (TEM), Fourier transform infrared spectrometry (FT-IR) and thermogravimetry (TG) techniques. The potential use of these bifunctionalized nanoparticles as pseudostationary phases (PSPs) in capillary electrophoresis (CE) for the separation of charged and neutral compounds was evaluated in terms of their suitability. As expected, fast separation of representative aromatic acids was fulfilled with high separation efficiency, because they migrate in the same direction with the electroosmotic flow (EOF) under optimum experimental conditions. Using a buffer solution of 30 mmol/L phosphate (pH 3.0) in the presence of 0.5 mg/mL of the synthesized bifunctionalized nanoparticles, the investigated basic compounds were baseline-resolved with symmetrical peaks. Due to the existence of amino groups on the surface of nanoparticles, "silanol effect" that occurs between positively charged basic analytes and the silanols on the inner surface of capillary was greatly suppressed. Furthermore, the separation systems also exhibited reversed-phase (RP) behavior when neutral analytes were tested.

1. Introduction

In recent years, silica-based functionalized nanoparticles have attracted more and more researching interest for many intriguing advantages they process, such as good biocompatibility, high organic solvent resistance and commercial availability [1]. Many scientists have focused on the potential conjunction of silica nanoparticles with separation science to optimize detection [2,3], facilitate separation of nanoparticles themselves [4–6] and dramatically improve resolution of target molecules [7–9]. Most applications for these purposes require that the utilized silica nanoparticles should possess high surface area and small particle size less than 100 nm to ensure high monodispersity. In many cases, the silica nanoparticles have to be surface coated or derivative with specific functional groups to provide additional interaction sites [10]. Achieving controlled localization of two or more different molecular functionalities on the surface of nanoparticles would offer several profound advantages in drug separation and other applications, such as tumor cell targeting and attaching large molecules [11–14]. Functional groups like thiol, amine and carboxyl groups [15] are the crucial elements for the surface modification.

Nanoparticles can be added in buffer solutions to act as pseudostationary phases (PSPs) in capillary electrophoresis (CE) [16,17] and chip-based CE systems [18,19]. Nanoparticle-based capillary electrophoresis (NPCE) [20] is an increasingly used strategy as an elegant alternative to capillary electrochromatography (CEC) in packed [21,22] or monolithic [23] columns and has been applied for the separation of small molecules [24], DNA [7] and a few cases of proteins [25]. When nanoparticles are used as PSPs, they are suspended in the electrolyte and are continuously pumped through the capillary by the electroosmotic flow (EOF) during separation. Nanoparticles used in NPCE usually include polymer nanoparticles [24], gold nanoparticles [7], molecularly imprinted polymer nanoparticles [17], dendrimers [26] and silica nanoparticles [8]. The research in this field has been reviewed by Nilsson and Nilsson [27] and Palmer [28] in detail, among which silica nanoparticles have been usually announced. For example, by using chemical modification method, Bächmann and Göttlicher covalently modified commercially available silica nanoparticles with a combination of reversed-phase groups and negatively charged groups [29]. In comparison with the sodium dodecyl sulfate (SDS) coated nanoparticles [30], the separation of larger PAHs was possible under a buffer solution with high amounts of organic modifiers added. Neiman et al

* Corresponding author.
E-mail address: Tanganna@nankai.edu.cn (A.-N. Tang).

0021-9673/$ – see front matter © 2010 Elsevier B.V. All rights reserved.
doi:10.1016/j.chroma.2010.09.050

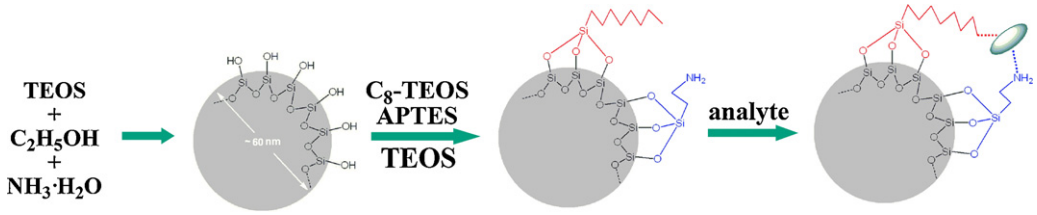

Fig. 1. Schematic diagram for the synthetic approaches of bifunctionalized nanoparticles.

prepared one neutrally charged and two positively charged organically modified silica sols for the CE separation of aromatic acids and their structural isomers [8]. Their experiments suggested that small changes in the functional groups on surface of silica nanoparticles had a pronounced effect on the interactions between the nanoparticles and the analytes.

Herein, we synthesized novel bifunctionalized amphiphilic silica nanoparticles with the average diameter of 60 nm using a modified Stöber method [31]. Three precursors, tetraethoxysilane (TEOS), aminopropyltriethoxysilane (APTES) and octyltriethoxysilane (OTES) were used for the fabrication. The surface of the obtained nanoparticles consists of octyl groups which are specially designed for RP interaction with the analytes, and charged amino groups which ensure the mobility of the particles in the electric field. Under optimum experimental conditions, some selected acidic, neutral and basic compounds were successfully separated based on different separation mechanisms. To the best of our knowledge, this is the first time for the preparation of silica nanoparticles containing both amino and octyl groups, which were further used as PSPs in NPCE.

2. Experimental

2.1. Reagents

All chemicals were analytical grade unless noted otherwise. Double-distilled water (DDW) purified by a Nanopure II system (Barnstead, USA) was utilized throughout the experiment. TEOS (98%), APTES (99%) and OTES (98%) were purchased from Guotai-Huarong New Chemical Materials (Zhangjiagang, China). Ammonia (28 wt%), ethanol, p-toluenesulfonic acid, p-aminobenzosulfonic acid, p-nitrobenzoic acid, nitrobenzene, phenol, aniline, propranolol, and pyridine were purchased from Tianda Kewei (Tianjin, China). Phosphoric acid, sodium hydroxide, sodium dihydrogen phosphate, and hydrochloric acid were from Tianjin Yuanli Chemicals (Tianjin, China).

2.2. Synthesis and characterization of amphiphilic nanoparticles

Amphiphilic nanoparticles were prepared by the modified Stöber method [31]. Fig. 1 shows the schematic reaction pathways for the preparation and co-condensation. A total amount of 2 mL of TEOS (~9 mmol) was added to a conical flask in the presence of 25 mL of EtOH and 0.8 mL of ammonia under stirring. After 24 h of reaction at room temperature, the functionalized trialkoxysilane reagents (with different volume ratios of APTES/OTES) were added with extra TEOS with the volume ratio of (APTES + OTES)/TEOS = 1:1 (Table 1) for particle co-condensation. The total amount of functionalized trialkoxysilane reagents (APTES + OTES) added corresponds to ~5% (~0.45 mmol) of the initial amount of TEOS. The obtained mixture reacted for another 24 h, and the particles thus formed were centrifuged and washed with ethanol and DDW repeatedly, then vacuum-dried at 80 °C for 6 h. For comparison, silica nanoparticles were prepared in the same way as that of bifunctionalized nanoparticles except that no functionalized reagents were added in the second step.

Scanning electron microscopy (SEM) and transmission electron microscopy (TEM) were carried out on a Shimadzu SS-550 microscope at 15.0 kV and a Philips Tecnai G20 at 200 kV, respectively. Fourier transform infrared (FT-IR) spectra were measured on a Bruker VECTOR 22 spectrometer with the KBr pellet technique, and the ranges of spectrograms were 4000–400 cm^{-1}. Thermogravimetry (TG) was performed using a TA SDT Q600 instrument at a heating rate of 2 °C/min in standard air using α-Al_2O_3 as the reference.

2.3. Instrumentation

All CE experiments were carried out on a TH-3000 HPCE-HPLC amphibious system equipped with a CXTH-3000 data handling software (Tianhui Instruments, Baoding, China). The detection wavelength was set at 214 nm unless stated otherwise. Fused-silica capillaries of 375 μm o.d. and 75 μm i.d. (Yongnian Optic Fiber Co., Hebei, China) were used throughout the experiment. A capillary with the total length (TL) of 36 cm and the effective length (EL) of 27 cm was made by scraping off 3–5 mm of the polymer outside the capillary at an appropriate place. Prior to the first use, the capillary was successively rinsed by methanol, DDW, 1 mol/L NaOH, DDW, 0.1 mol/L HCl, DDW and buffer solution for 15 min each. The EOF was determined by using thiourea as the neutral marker unless stated otherwise.

2.4. Buffer solution

Stock solution of 200 mmol/L phosphate buffer was prepared by dissolving a certain amount of sodium dihydrogen phosphate in DDW. Prior to use, it was diluted to the desired concentration and adjusted to the appropriate pH value with 1 mol/L NaOH or concentrated H_3PO_4. Sample solutions were prepared at proper concentrations before injection. All the stock solutions were kept at 4 °C in a refrigerator. Before use, all solutions were filtered through a 0.45 μm nylon membrane and degassed by ultrasonication.

Table 1
Compositions of the derivatization reagents used for the modification.

Nanoparticles	TEOS (μL)	APTES (μL)	OTES (μL)	APTES/OTES (volume ratio)	APTES/OTES (molar ratio)
I	100	10	90	1:9	1:6.70
II	100	30	70	3:7	1:1.74
III	100	50	50	1:1	1:0.74

3. Results and discussion

3.1. Formation of amphiphilic nanoparticles

Generally speaking, two pathways are available in synthesizing organosilica materials, namely, post-grafting (the subsequent surface-modification of pure nanoparticles) and co-condensation (the simultaneous condensation of inorganic silica and organosilica precursors). However, the co-condensation approach is better than post-grafting for the introduction of organosilica in terms of a high and uniform surface coverage of organic units [32].

As shown in Fig. 1, the preparation of amphiphilic silica nanoparticles was accomplished by a modified Stöber method [31]. Firstly, ammonia solution was used as the basic catalyst to catalyze the TEOS sol–gel process based on Stöber theory [33]. The second step involves the introduction of the functional groups by condensation reaction of TEOS, APTES and OTES with the silanols on the surface of the previously formed silica nanoparticles. According to the APTES/OTES volume ratios (Table 1) used in the second step, up to three particle populations differing in surface functional group density were obtained (named as nanoparticles I, II and III, respectively).

Recently, Bagwe et al. [34] carried out a systematic study of the design and development of surface-modification schemes for silica nanoparticles. It was found in their research that amine-modified silica nanoparticles tended to aggregate in weakly acidic solution for the existence of electrostatic interactions between positively charged amino groups and negatively charged silanol groups. To achieve minimal nanoparticles aggregation, the simultaneous use of inert and active surface functional groups should be advocated. This rule is well obeyed in our research where active APTES and inert OTES are used as surface functional groups. As a result, nanoparticles with good monodispersity and homogeneous size are obtained.

3.2. Characterization of amphiphilic nanoparticles

Although having different surface functional group densities, bifunctionalized nanoparticles I, II and III present nearly same morphology as to the shape and size. The SEM (a) and TEM (c) images of the synthesized nanoparticles II, and the SEM (b) image of pure silica nanoparticles are shown in Fig. 2. It can be seen that the prepared materials are sphere-like and uniform in shape with the size of about 60 nm.

FT-IR spectra of pure silica nanoparticles and bifunctionalized amphiphilic nanoparticles II are presented in Fig. 3. In comparison with that of pure silica nanoparticle, several newborn absorption bands appeared in the spectrum of bifunctionalized nanoparticles II. The peaks at 2950 and 2850 cm^{-1} are asymmetric stretching vibration and symmetric stretching vibration of C–H, respectively. The double peaks between 3300 and 3500 cm^{-1} are assigned to the stretching vibration of amino group (ν_{-NH2}), and the peaks at 1650 and 611 cm^{-1} are the bending vibration of amino group (δ_{-NH2} and τ_{-NH2}). Another peak at 1396 cm^{-1} corresponds to the bending vibration of C–H (δ_{-CH3}).

The C and N contents for the obtained materials were determined by elemental analysis to roughly estimate the NH_2/C8 ratios (Table 2). Although the ratios are not exactly the same as those of

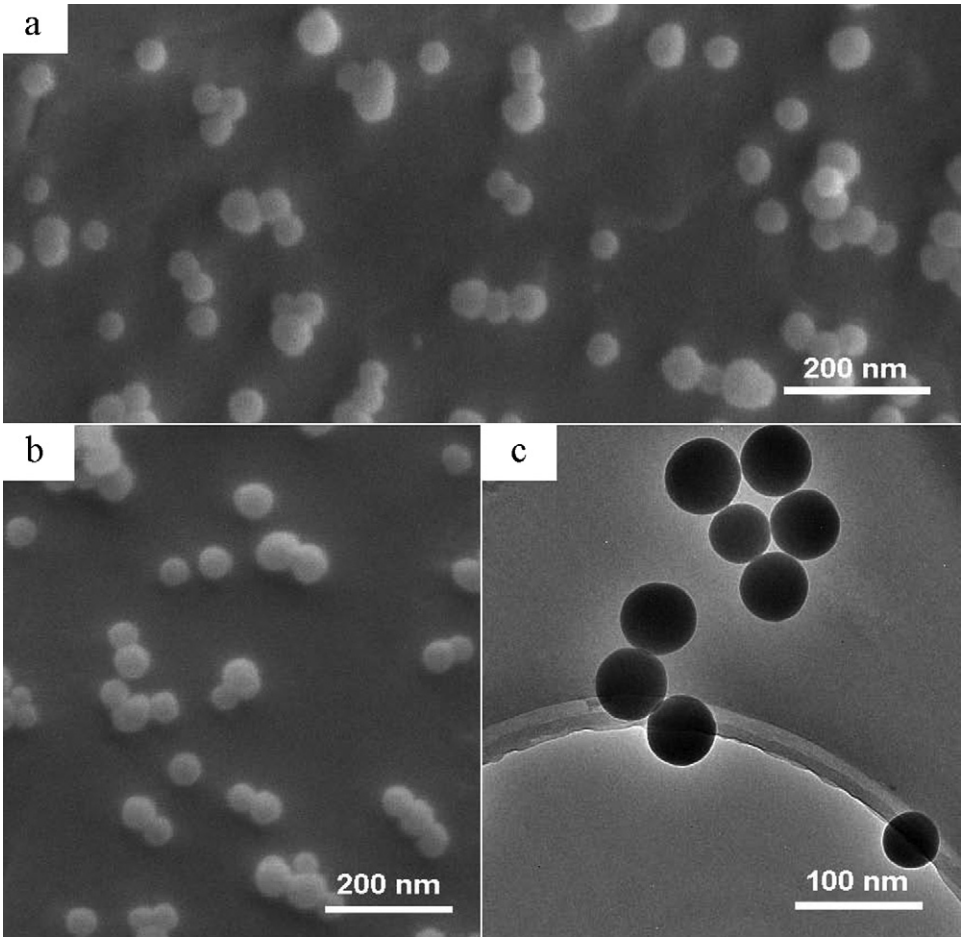

Fig. 2. SEM images of nanoparticles II (a), pure silica nanoparticles (b) and TEM image of nanoparticles II (c).

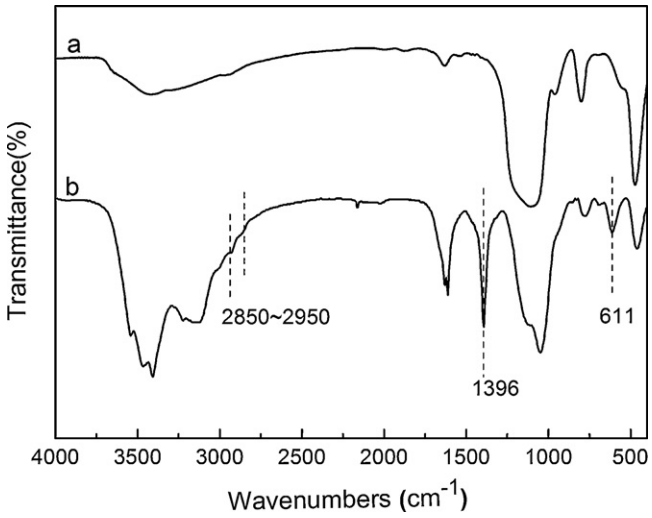

Fig. 3. The IR spectra of pure silica nanoparticles (a) and nanoparticles II (b).

Table 2
Elementary analysis of nanoparticles I, II and III.

Nanoparticles	C (%)	N (%)	NH_2/C_8 (molar ratio)
I	5.13	0.11	1:6.43
II	3.73	0.26	1:1.72
III	3.08	0.42	1:0.69

the reactants (Table 1), the increased tendency from nanoparticles I to III is obvious which is in accordance with the added reactants.

TG curves of the bifunctionalized nanoparticles II and pure silica nanoparticles are given in Fig. 4. By comparison, it can be deduced that the weight loss below 180 °C is assigned to the evaporation of adsorbed ethanol and water, and the weight decrease between 180 °C and 750 °C is related to the decomposition of organic groups (aminopropyl and octyl groups) and the condensation of silanol groups (dehydroxylation). The obvious weight loss in the range of 440–550 °C for bifunctionalized nanoparticles offers evidence that the second step, namely, functional groups modification process, is successful.

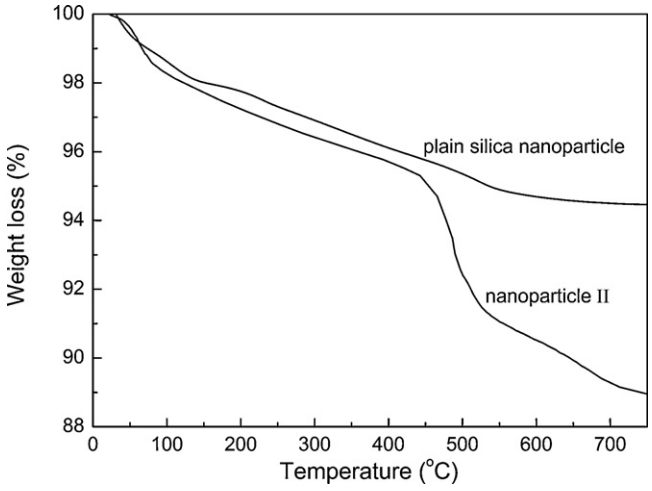

Fig. 4. TG curves of pure silica nanoparticles (a) and nanoparticles II (b).

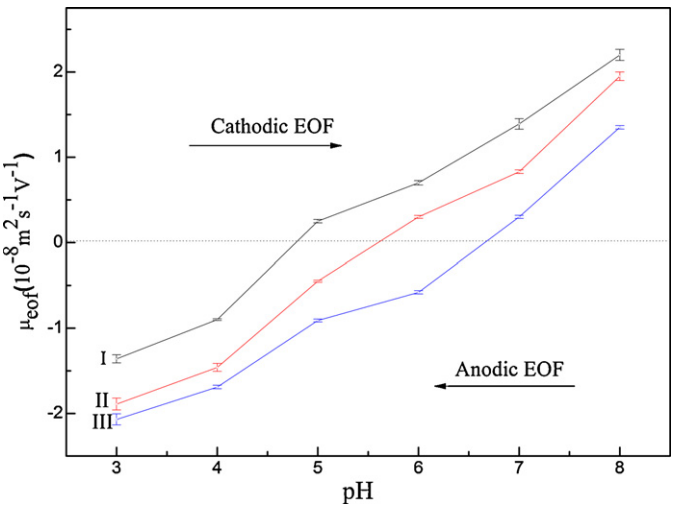

Fig. 5. The effect of buffer pH on EOF. Experimental conditions: capillary, total length 36 cm, effective length 27 cm; buffer, 30 mmol/L phosphate buffer with 0.5 mg/mL amphiphilic silica nanoparticles; detection wavelength, 214 nm; polarity voltage, −12 kV or 12 kV; injection, 8 kV × 3 s.

3.3. EOF characteristic

EOF is a very important factor in CE separation because analytes move through the capillary by EOF drive, as well as self-electrophoretic mobility if they are charged. Knowing the characteristics of the EOF will be helpful to understand the separation behavior, and furthermore, to select optimal separation conditions. The EOF was measured by using thiourea as the neutral marker, and calculated as follows:

$$\mu_{eof} = \frac{lL}{tV}$$

where μ_{eof} is the EOF mobility; l and L are the effective length (27 cm) and the total length (36 cm) of the capillary, respectively; t is the migration time taken by thiourea to migrate from the inlet to the detection window; and V is the voltage applied across the capillary column. Since the direction of EOF was unknown when nanoparticles were present in different buffer solutions, tentative experiments were necessarily made. Firstly, a positive polarity voltage (+12 kV) was applied across the capillary, i.e., thiourea was injected from the anode end. If no signal was observed in 2 h, thiourea was then injected from the cathode end and a negative polarity voltage (−12 kV) was applied. In this way, the direction (cathodic or anodic) and magnitude of EOF were confirmed ultimately. Considering the fact that silica-based materials tend to dissolve in strongly alkaline solutions, we selected the pH range of 3–8 for investigation.

Fig. 5 shows the plots of electroosmotic mobility versus pH of the buffer solutions containing three types of bifunctionalized nanoparticles. Very similar plots were obtained, i.e., cathodic and anodic EOF was observed under certain buffer conditions. From Fig. 5, it can be observed that the reversed anodic EOF increased in the order of nanoparticles I, II and III, which is in accordance with the compositions of the modification reagents shown in Table 1.

Recently, Ding et al. [35] reported the preparation of a mixed-mode silica-based monolithic column with amino and octyl groups in the network. The capillary monolithic column generated anodic EOF in the pH range of 3.0–7.5 due to the protonation of amino groups. Using polystyrene particles derivative with ethylenediamine (or 1, 10-diaminodecane) as CE buffer additive, Kleindienst et al. [36] obtained a stable and irreversibly adsorbed coating, and used it for the separation of basic and acidic proteins with high efficiencies. Since the bifunctionalized nanoparticles contain amino

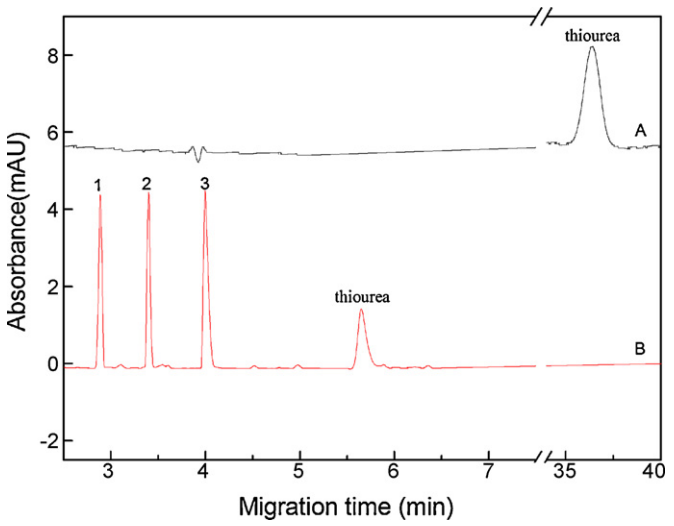

Fig. 6. The electropherograms of three acidic compounds in the absence (A) and in the presence of nanoparticles II (B). Experimental conditions: capillary, total length 36 cm, effective length 27 cm; buffer, 30 mmol/L phosphate buffer (pH 3.0) with (or without) 0.5 mg/mL nanoparticles II added; detection wavelength, 214 nm; polarity voltage, 12 kV (A) or −12 kV (B); injection, 8 kV × 3 s. Peak identities: (1) *p*-toluenesulfonic acid (p*K*a 1.7); (2) *p*-nitrobenzoic acid (p*K*a 3.44); (3) *p*-aminobenzosulfonic acid (p*K*a 3.24).

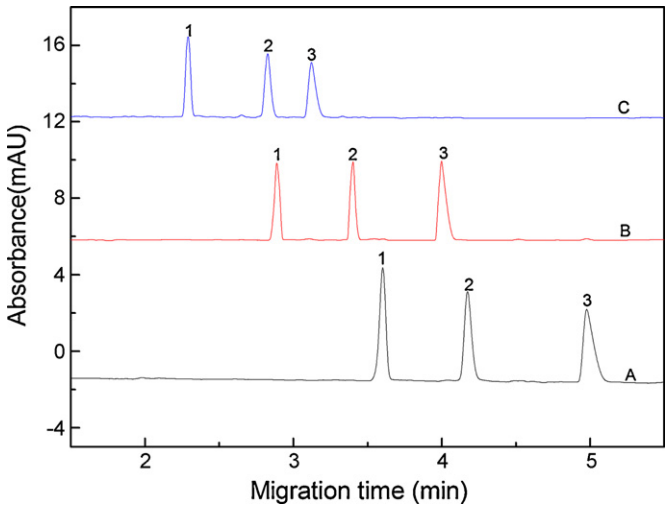

Fig. 7. The electropherograms for the separation of acidic compounds in the presence of nanoparticles I (A), nanoparticles II (B) and nanoparticles III (C). The other conditions are the same as mentioned in Fig. 6.

groups on the surface, it is not surprising that they will be positively charged and adsorbed on the inner surface of capillary to form a dynamic coating under acidic buffer solutions, and as a result, reversed anodic EOF was obtained accordingly.

Taking nanoparticles II as an example, the stability of separation system was investigated by using thiourea as the analyte. For 20 times of repeating injections in the same day, relative standard deviation (RSD) for the migration time of thiourea was 1.13%, which indicates a relatively good stability of the separation system. Further experiments showed that the RSDs ($n = 5$) for the migration of the thiourea in the batch-to-batch and day-to-day were 2.64% and 2.17%, respectively.

3.4. Separation of acidic compounds

The separation of acidic compounds in bare capillary is often unsatisfactory because acidic compounds migrate in the reverse direction with the EOF, resulting in longer separation time [37]. For fast and efficient separation of acidic compounds, it is preferred that the analytes migrate in the same direction with the EOF (*co*-EOF). Since the direction of EOF is from cathode to anode under lower pH conditions in present separation system (Fig. 5), it is expected that fast separation can be obtained for acidic compounds. Fig. 6 shows the electropherograms for the separation of three acidic compounds under different conditions. For clarity, thiourea was added in the mixed sample to act as the neutral marker. When nanoparticles were not added in buffer solutions, acidic compounds were eluted very slowly and no peaks of acidic compounds were observed in 1 h due to the EOF was very weak (Fig. 6A). When nanoparticles were added in the same buffer solutions, the situation was quite different, i.e., all of the acidic compounds were baseline separated in less than 5 min with high separation efficiency (Fig. 6B).

When charged compounds are separated in CE system, the mechanism for the separation may be complicated. Since the elution order of acidic compounds was not in the order of their p*K*a values, it can be deduced that hydrophobicity and weak anion exchange may also participate in the separation process as well as electrophoretic mobility considering that nanoparticles used here were bifunctionalized. The electropherograms for the separation of acidic compounds in the presence of three different kinds of nanoparticles were shown in Fig. 7. It was found that with the increasing of the amount of amino groups on the surface of nanoparticles from I to III, the migration times of acidic compounds were shortened accordingly. The above experimental results suggest a new method to tune and control EOF and the migration time of analyzed compounds, that is, by utilizing functionalized nanoparticles with different ratios of functional groups.

The reproducibility of migration times and peak areas of acidic compounds in a single capillary was determined from 5 consecutive runs. The measured RSDs of migration times and peak areas were 1.46% and 2.67%, respectively, which indicated that the present method had good reproducibility and could be used in qualitative and quantitative analysis.

Considering the fact that nanoparticles II offer the optimum separations for acidic compounds in relation to resolution and column performance (Fig. 7), nanoparticles II were selected to investigate the effect of the nanoparticles concentration on the separation of organic acids. The results are shown in Fig. 8. It should be noted that

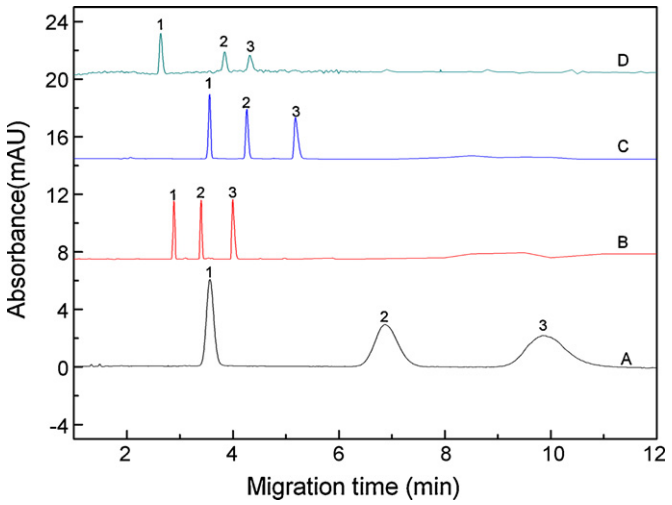

Fig. 8. The effect of nanoparticles II concentration on the separation of three organic acids. Experimental conditions: buffer, 30 mmol/L phosphate buffer (pH 3.0) with nanoparticles II added (A) 0.25 mg/mL; (B) 0.5 mg/mL; (C) 1.0 mg/mL; (D) 2.0 mg/mL. The other conditions are the same as mentioned in Fig. 6.

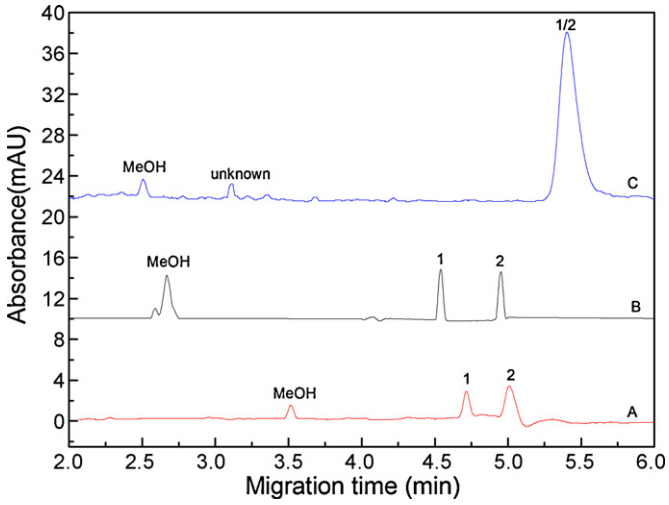

Fig. 9. The electropherograms for the separation of neutral compounds in the presence of nanoparticles I (A), nanoparticles II (B) and nanoparticles III (C). Experimental conditions: buffer, 30 mmol/L phosphate buffer (pH 3.0) with 0.5 mg/mL nanoparticles added; and other conditions are the same as mentioned in Fig. 6. Peak identities: (1) phenol; (2) nitrobenzene.

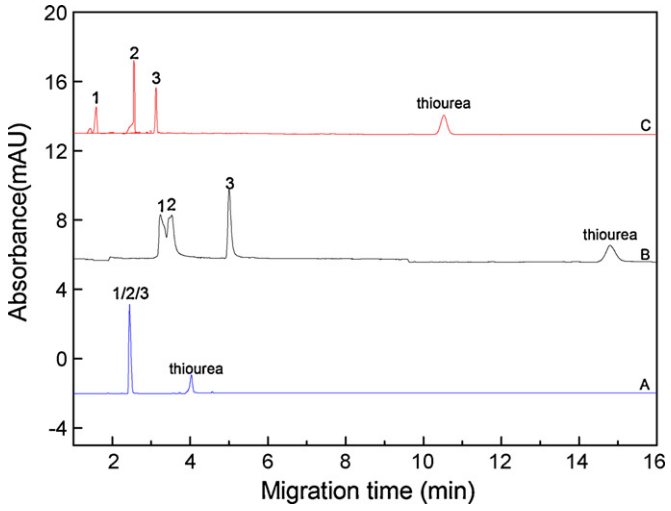

Fig. 10. The electropherograms for the separation of basic compounds on bare capillary (A), in the presence of pure silica nanoparticles (B) and nanoparticles II (C). Experimental conditions: buffer, 30 mmol/L phosphate buffer (pH 6.0) with (or without) 0.5 mg/mL nanoparticles added; polarity voltage, 12 kV; injection, 8 kV × 3 s; and other conditions are the same as mentioned in Fig. 6. Peak identities: (1) *o*-toluidine; (2) propranolol; (3) pyridine.

the EOF was from cathode to anode in all cases. With the increasing of the nanoparticles concentration from 0.25 to 2.0 mg/mL, the analysis time was usually shortened and the separation performance was improved. However, a disadvantageous phenomenon was also observed at the same time, i.e., the detection sensitivity was lowered with the increasing of the amount of nanoparticles in buffer solutions, probably due to aggregation and light scattering of nanoparticles. As a compromise, nanoparticles concentration of 0.5 mg/mL was ultimately selected for further experiments.

3.5. Separation of neutral compounds

As discussed in Section 3.3, bifunctionalized nanoparticles can be regarded as a dynamic coating when they were added in proper buffer solutions. Considering the fact that hydrophobic octyl groups exist on the surface of nanoparticles, hydrophobic interactions may take place between analytes and nanoparticles. Fig. 9 shows the separation results of several neutral compounds in buffer solutions containing different bifunctionalized nanoparticles. The methanol used as the EOF marker migrates faster than the other neutral solutes. The elution order (migration time) of methanol < phenol < nitrobenzene suggests the hydrophobicity mechanism (Fig. 9A, B). Nanoparticles III were also tested for these compounds. However, no separation was achieved probably due to the weakest hydrophobicity of nanoparticles III among the three kinds of nanoparticles prepared (Fig. 9C). Using nanoparticles II as an example, we also investigated their effective electrophoretic mobility (μ_{ef}) of free nanoparticles (i.e., nanoparticles not adsorbed on the capillary surface) in the separation system through injecting a segment of solution containing nanoparticles II with higher concentration (e.g., 3.0 mg/mL). It was found experimentally that nanoparticles still migrated from cathode to anode although the migration rate was very slow. According to equation $\mu_{ap} = \mu_{ef} + \mu_{EOF}$, we calculated the μ_{ef} of nanoparticles II to be 0.24×10^{-8} m^2 s^{-1} V^{-1}, which is in accordance with their surface charges, i.e., positively charged under acidic running buffer conditions.

To the best of our knowledge, there are only few papers reporting on the separation of neutral compounds using silica-based nanoparticles [8,29]. Using APTES sol as buffer additive, Neiman et al. [8] separated nitrobenzene and its structural analogs under low pH buffer solution. Although the separation conditions are not totally same, it is obvious that our results are better in both analysis time and separation performance by comparing the obtained electropherograms with those in the previously reported works (Fig. 9B).

3.6. Separation of basic compounds

In most cases, it is favorable to get the peaks off the capillary as quickly as possible to obtain high column performance, especially in free-zone electrophoresis mode. However, when strongly basic compounds are investigated, *co*-EOF electrophoresis conditions often lead to limited separation time window, resulting in the overlapping of electrophoretic peaks (Fig. 10A). Furthermore, the interaction between the negatively charged inner surface of capillary and the positively charged analytes may result in severe peak tailing. To circumvent this problem, coated capillary columns and amphiphilic CEC columns were fabricated and widely used in the past decades [38,39]. However, the fabrications were usually involved in multi-step and time-consuming processes, resulting in poor column to column reproducibility.

The separations of basic compounds of *o*-toluidine, propranolol and pyridine under NPCE mode are shown in Fig. 10 under different separation conditions. Since three nanoparticles are all amphiphilic and positively charged in the running buffer, and nanoparticles II offer the optimum separations for acidic and neutral compounds in relation to resolution and column performance (Figs. 7 and 9), nanoparticles II were selected as a representative for the separation of basic compounds in comparison with pure silica nanoparticles (Fig. 10). Although the separation selectivity was largely improved when pure silica nanoparticles were added in buffer solution, the result was not satisfactory for *o*-toluidine and propranolol were not baseline-resolved (Fig. 10B). In comparison with pure silica nanoparticles (Fig. 10B), symmetrical peaks and satisfactory separation for tested compounds were obtained with bifunctionalized nanoparticles II (Fig. 10C) for the positively charged amino groups minimized the adsorption of the positively charged analytes to the inner surface of capillary.

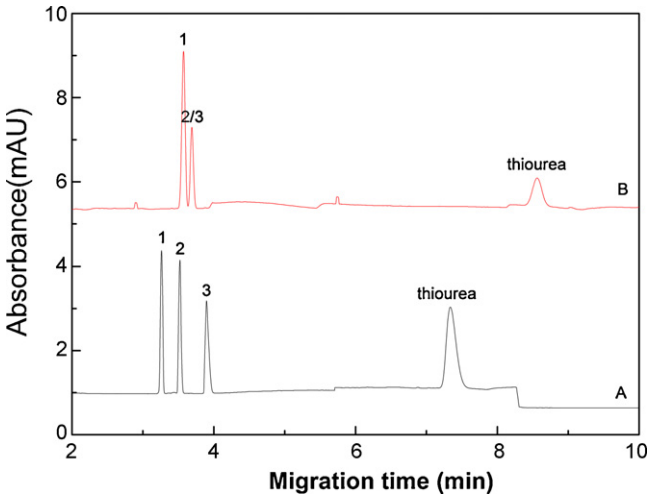

Fig. 11. The separation of acidic compounds in the first (A) and second (B) hour after the replacement of running buffer. Experimental conditions: buffer, 30 mmol/L phosphate buffer (pH 3.0) in the absence of nanoparticles II. The other conditions are the same as mentioned in Fig. 6.

3.7. Functionalities of amphiphilic nanoparticles

When different types of nanoparticles were added into the running buffer, they could be kinetically adsorbed onto the inner wall of capillary to change (or reverse) EOF. As separation media, nanoparticles could also participate in the separation process acting as PSPs to improve the separation efficiency and selectivity [1,27,36].

As shown above, the newly prepared bifunctionalized nanoparticles can be successfully used for the separation of charged analytes, i.e., acidic and basic compounds through reversing (or restraining) EOF. To testify the formation of a dynamic coating under acidic buffer solutions, we carried out an interesting experiment. It should be noted that prior to the experiment, the capillary was unlimitedly flushed with running buffer containing 0.5 mg/mL nanoparticles II for more than 0.5 h using syringe. It was found experimentally that anodic EOF would last for several hours after replacing the nanoparticles containing running buffer with the running buffer without nanoparticles, which testifies the existence of the adsorbed coating. The separations of acidic compounds in the first (A) and second (B) hour after the replacement of running buffer are shown in Fig. 11. From these experimental results, it can be conclude that the adsorbed coating is reversible and its existence is very important for the highly effective separation of acidic compounds.

Similar experiments were also carried out for neutral compounds. However, tested neutral compounds eluted at the same time and no separation was obtained even in the first hour after the replacement of running buffer. The results imply the importance of free nanoparticles in running buffer, which act as PSPs to participate in the separation process of neutral compounds.

4. Conclusion

In this research, amphiphilic silica nanoparticles surface-bonded with amino and octyl groups, were successfully synthesized and used under NPCE mode for the separation of charged and neutral compounds. The experimental results showed that there were great improvements in the separation selectivity and efficiency in comparison with the traditional CE method. Fast and efficient separation of aromatic acids was achieved by using an acidic buffer under *co*-EOF conditions. Basic compounds were baseline-resolved with symmetrical peak shapes under suppressed EOF conditions for the positively charged amino groups restrained the adsorption of the positively charged analytes to the inner surface of capillary to a certain degree. Due to the existence of hydrophobic octyl groups, selected neutral compounds were also separated based on reversed-phase mechanism. Further work will be focused on the investigation of the interaction mechanism of bifunctionalized nanoparticles in different separation systems. The separation of samples of biological interest, such as plant hormones, proteins and DNA using silica-based nanoparticles surface-modified with various functional groups is also under way.

Acknowledgements

Financial support from Nation Nature Science Foundation of China (20505011 and 21005054) and National Basic Research Program of China (2011CB707703) is gratefully acknowledged.

References

[1] Y.Q. Wang, W.R.G. Baeyens, C.G. Huang, G.T. Fei, H. Li, J. Ouyang, Talanta 77 (2009) 1667.
[2] M.J.A. Shiddiky, Y.B. Shim, Anal. Chem. 79 (2007) 3724.
[3] M. Pumera, J. Wang, E. Grushka, R. Polsky, Anal Chem. 73 (2001) 5625.
[4] X. Song, L. Li, H. Qian, N. Fang, J. Ren, Electrophoresis 27 (2006) 1341.
[5] Y. Wang, J. Ouyang, W.R.G. Baeyens, J.R. Delanghe, Exp. Rev. Prot. 4 (2007) 287.
[6] F.K. Liu, M.H. Tsai, Y.C. Hsu, T.C. Chu, J. Chromatogr. A 1133 (2006) 340.
[7] M.F. Huang, Y.C. Kuo, C.C. Huang, H.T. Chang, Anal. Chem. 76 (2004) 192.
[8] B. Neiman, E. Grushka, O. Lev, Anal. Chem. 73 (2001) 5220.
[9] C. Nilsson, P. Viberg, P. Spegel, M. Jornten-Karlsson, P. Petersson, S. Nilsson, Anal. Chem. 78 (2006) 6088.
[10] A.K. Gupta, M. Gupta, Biomaterials 26 (2005) 3995.
[11] V. Cauda, A. Schlossbauer, J. Kecht, A. Zürner, T. Bein, J. Am. Chem. Soc. 131 (2009) 11361.
[12] C.Y. Lai, B.G. Trewyn, D.M. Jeftinija, K. Jeftinija, S. Xu, S. Jeftinija, V.S.Y. Lin, J. Am. Chem. Soc. 125 (2003) 4451.
[13] Y.S. Lin, C.P. Tsai, H.Y. Huang, C.T. Kuo, Y. Hung, D.M. Huang, Y.C. Chen, C.Y. Mou, Chem. Mater. 17 (2005) 4570.
[14] I.I. Slowing, B.G. Trewyn, V.S.Y. Lin, J. Am. Chem. Soc. 128 (2006) 14792.
[15] L. Wang, K.M. Wang, S. Santra, X.J. Zhao, L.R. Hilliard, J.E. Smith, Y.R. Wu, W.H. Tan, Anal. Chem. 78 (2006) 646.
[16] P. Viberg, M. Jornten-Karlsson, P. Petersson, P. Spégel, S. Nilsson, Anal. Chem. 74 (2002) 4595.
[17] P. Spégel, L. Schweitz, S. Nilsson, Anal. Chem. 75 (2003) 6608.
[18] M. Pumera, J. Wang, E. Grushka, R. Polsky, Anal. Chem. 73 (2001) 5625.
[19] V. Dolník, Electrophoresis 25 (2004) 3589.
[20] C. Nilsson, I. Harwigsson, K. Becker, J.P. Kutter, S. Birnbaum, S. Nilsson, Electrophoresis 31 (2010) 459.
[21] J.W. Jorgenson, K.D. Lukacs, J. Chromatogr. 218 (1981) 209.
[22] V. Pretorius, B.J. Hopkins, J.D. Schieke, J. Chromatogr. 99 (1974) 23.
[23] S. Eeltink, F. Svec, Electrophoresis 28 (2007) 137.
[24] R.A. Wallingford, A.G. Ewing, Adv. Chromatogr. 29 (1989) 1.
[25] C. Nilsson, K. Becker, I. Harwigsson, L. Bulow, S. Birnbaum, S. Nilsson, Anal. Chem. 81 (2009) 315.
[26] N. Tanaka, T. Tanigawa, K. Hosoya, K. Kimata, T. Araki, S. Terabe, Chem. Lett. 21 (1992) 959.
[27] C. Nilsson, S. Nilsson, Electrophoresis 27 (2006) 76.
[28] C.P. Palmer, Electrophoresis 25 (2004) 4086.
[29] K. Bächmann, B. Göttlicher, Chromatographia 45 (1997) 249.
[30] K. Bächmann, B. Göttlicher, I. Haag, K.Y. Han, W. Hensel, A. Mainka, J. Chromatogr. A 688 (1994) 283.
[31] C.A.R. Costa, C.A.P. Leite, F. Galembeck, J. Phys. Chem. B 107 (2003) 4747.
[32] X.B. Liu, Y. Du, Z. Guo, S. Gunasekaran, C.B. Ching, Y. Chen, S.S.J. Leong, Y.H. Yang, Micropor. Mesopor. Mater. 122 (2009) 114.
[33] W. Stöber, A. Fink, E. Bohn, J. Colloid Interface Sci. 26 (1968) 62.
[34] R.P. Bagwe, L.R. Hilliard, W.H. Tan, Langmuir 22 (2006) 4357.
[35] G.S. Ding, Z.L. Da, R.J. Yuan, J.J. Bao, Electrophoresis 27 (2006) 3363.
[36] G. Kleindienst, C.G. Huber, D.T. Gjerde, L. Yengoyan, G.K. Bonn, Electrophoresis 19 (1998) 262.
[37] M.L. Ye, H.F. Zou, Z. Liu, J.Y. Ni, J. Chromatogr. A 887 (2000) 223.
[38] M.W. Kamande, K.A. Fletcher, M. Lowry, I.M. Warner, J. Sep. Sci. 28 (2005) 710.
[39] D. Allen, Z. El Rassi, Electrophoresis 24 (2003) 3962.